Alternating current characterization of nano-Pt(II) octaethylporphyrin (PtOEP) thin film as a new organic semiconductor

M Dongol[1], M M El-Nahass[2], A El-Denglawey[1,3,†], A A Abuelwafa[1,4], and T Soga[4]

[1] *Nano and Thin Film Laboratory, Physics Department, Faculty of Science, South Valley University, Qena* 83523, *Egypt*

[2] *Physics Department, Faculty of Education, Ain Shams University, Roxy, Cairo* 11757, *Egypt*

[3] *Physics Department, Faculty of Applied Medical Science, Taif University, Turabah* 21995, *Kingdom of Saudi Arabia*

[4] *Department of Frontier Materials, Nagoya Institute of Technology, Gokiso-cho, Showa-ku, Nagoya* 466-8555, *Japan*

(Received 31 October 2015; revised manuscript received 24 January 2016; published online 25 April 2016)

Alternating current (AC) conductivity and dielectric properties of thermally evaporated Au/PtOEP/Au thin films are investigated each as a function of temperature (303 K–473 K) and frequency (50 Hz–5 MHz). The frequency dependence of AC conductivity follows the Jonscher universal dynamic law. The AC-activation energies are determined at different frequencies. It is found that the correlated barrier hopping (CBH) model is the dominant conduction mechanism. The variation of the frequency exponent s with temperature is analyzed in terms of the CBH model. Coulombic barrier height W_m, hopping distance R_ω, and the density of localized states $N(E_F)$ are valued at different frequencies. Dielectric constant $\varepsilon_1(\omega,T)$ and dielectric loss $\varepsilon_2(\omega,T)$ are discussed in terms of the dielectric polarization process. The dielectric modulus shows the non-Debye relaxation in the material. The extracted relaxation time by using the imaginary part of modulus (M'') is found to follow the Arrhenius law.

Keywords: PtOEP thin films, AC conductivity, dielectric constants, organic semiconductors, solar cell, nano materials

PACS: 72.15.v, 72.20.–i, 73.63.b, 73.50.h **DOI:** 10.1088/1674-1056/25/6/067201

1. Introduction

Organic semiconductors are comprised of organic materials such as organic oligomers, polymers and small organic molecules, which are formed by a π-conjugated system.[1] They are easily processed due to their flexibility, light weight, and low sublimation point. Band theory is used to describe the electronic transitions of organic and inorganic semiconductors. More detailed descriptions of the highest occupied molecular orbital (HOMO $\pi-$orbitals) and the lowest unoccupied molecular orbital (LUMO; π*-orbitals) and their relations with the valence and conduction band of inorganic semiconductors are available everywhere.[1–6]

Porphyrin has a wide range of variable properties because of its stability, free base and its two active positions, meso and beta. The free base of porphyrin can be combined with metals such as Mg, Fe, Zn, Ni, Co, Cu, Zn, and Pt to form metalloporphyrin.[2,7,8] Of course, metallo-porphyrin has different properties. Metalloporphyrin is considered to be a promising organic material, and it has many applications such as gas sensors, solar cell and photo voltaic systems, data storage media, optoelectronic devices and biological applications.[9–12] Owing to the limitations and hazards of the available organic materials and because of the dramatic increase of the industrial sectors of nanomaterials and nanotechnology, new organic materials with high quality and new properties, new researches are needed to solve these problems. Platinum octaethylporphyrin metalloporphysin or (PtOEP) is one of the newest promissing organic materials in the mentioned fields. So it is important to understand the nature of the conduction mechanism[13–15] to obtain the information about the interior of PtOEP in the region of relatively low conductivity and distinguish between localized and free band conduction.[16] Furthermore, dielectric relaxation studies are also important for understanding the nature and the origin of dielectric losses, which in turn may be useful for determining the structures and defects in solids.[17]

Various models have been proposed to explain the AC conductivity.[13–17] Many studies of porphyrin derivatives: H_2TPP,[18] FeTPPCl,[19] CoMTPP,[20] and CuTPP[21] NiTPP[7,8,22] were performed. Platinum octaethylporphyrin (PtOEP) nanostructure and optical properties were studied through our earlier work.[23,24] According to the available literature, AC conduction mechanism and dielectric properties of thermally evaporated PtOEP thin film have not been reported

†Corresponding author. E-mail: denglawey@lycos.com

© 2016 Chinese Physical Society and IOP Publishing Ltd

yet. The present work focuses on the effects of temperature (303 K–473 K) and applied frequencies (50 Hz–5 MHz) on the electrical conductivity of PtOEP film respectively. Moreover, dielectric constants and complex dielectric modulus of PtOEP thin film are also studied.

2. Experimental details

2.1. Preparation of samples

Pt(II)octaethylporphyrin (PtOEP) powder provided by Aldrich was used to prepare 220-nm thick PtOEP films by using an Edwards E306A coating unit. Film thickness and deposition rate were controlled by using a quartz crystal thickness monitor (Edwards, FTM5) and confirmed by Tolansky's interferometric technique.[25] The schematic diagram of the molecular structure of PtOEP is shown in Fig. 1.

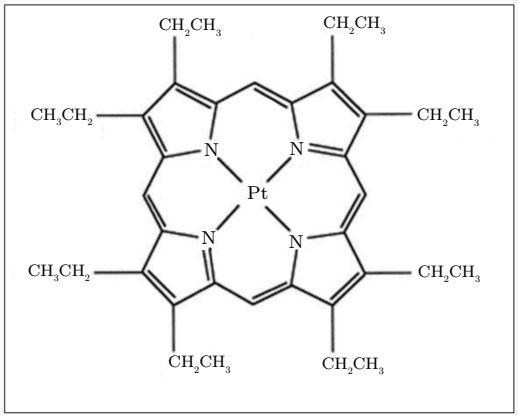


Fig. 1. The molecular structure of PtOEP.

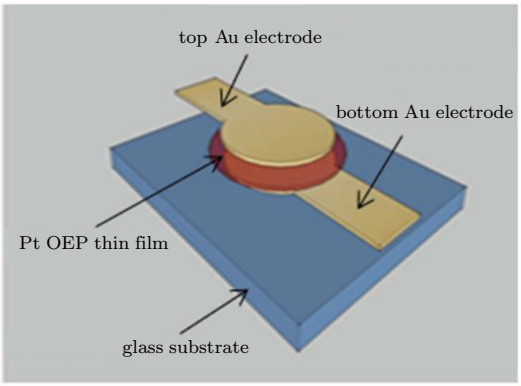


Fig. 2. (color online) The structure diagram of Au/PtOEP /Au.

The Au/PtOEP/Au sandwich structure was used to investigate the alternating current (AC) electrical properties as indicated in Fig. 2. The layer thickness values of the mentioned design were 100, 220, and 100 nm, respectively. The PtOEP deposition process was performed at a deposition rate 0.3 nms^{-1} and vacuum of 10^{-6} Torr (1 Torr $= 1.33322 \times 10^2$ Pa), and a deposition rate of 0.5 nms^{-1} for the gold electrode. The lower and upper gold electrodes were deposited through masks, they were circular in shape each with an effective area of 0.20 cm^2. The two-point probe technique was used to measure AC conductivity. All measurements of PtOEP thin films were performed in air and dark conditions, separately. A NiCreNiAl thermocouple with an accuracy of ± 1 K was used to measure the sample temperature. AC electrical measurements were performed by using a programmable automatic LCR Bridge (model Hioki 3532-50 Hitester).

2.2. AC electrical measurements

Total electrical conductivity $\sigma(\omega)$, dielectric constant ε_1, and dielectric loss ε_2 of PtOEP film were calculated respectively according to[14,26]

$$\sigma_{\mathrm{ac}}(\omega) = \sigma(\omega) - \sigma_{\mathrm{dc}}, \tag{1}$$

where σ_{dc} is the dc conductivity, which is independent of frequency. Its value can be obtained by extrapolating the experimental data of $\sigma(\omega)$ at low frequency down to zero value, and σ_{ac} is the frequency-dependent conductivity. $\sigma(\omega)$ can be calculated from

$$\sigma(\omega) = \frac{d}{ZA}, \tag{2}$$

where d is the film thickness, A is the cross-sectional area, and Z is the impedance

$$\varepsilon_1 = \frac{Cd}{\varepsilon_0 A}, \tag{3}$$

where ε_0 is the permittivity of free space.

$$\varepsilon_2 = \varepsilon_1 \tan\delta, \tag{4}$$

where $\tan\delta$ ($\delta = 90 - \phi$) is the dissipation factor.

The frequency-dependent AC electrical conductivity, σ_{ac} can be expressed by the following equation[27,28]

$$\sigma_{\mathrm{ac}}(\omega) = A\omega^s, \tag{5}$$

where ω is the angular frequency, A and s are the frequency and exponent factor both of which are temperature-dependent parameters. The frequency exponent s is obtained by least squares straight-line fit of the experimental data and is plotted as a function of temperature. There are many theoretical models proposed to explain the conduction mechanism of σ_{ac} with $s(T)$ behavior, i.e., the quantum-mechanical tunneling (QMT) model, small polaron tunneling (SPT) model, large polaron tunneling (LPT) model, atomic hopping (AH) model, and correlated barrier hopping (CBH) model.[27,29] The CBH model is a dominant conduction mechanism in our obtained data.

The value of s is in a range from 0.7 to 1.0 at room temperature, and decreases with increasing temperature according to CBH.

In the CBH model,[27–30] the conduction mechanism occurs via a bipolaron hopping process. It was concluded that

two electrons simultaneously hop over the potential barrier, this hopping occurs between two charged defect states (D^+ and D) and Coulombic interaction controls the correlation between the barrier height and the intersite separation. At high temperatures, thermal excitations of D^+ and D^- states and single polaron hopping produce D states.

The exponent s was found to obey the following equation[29]

$$s = 1 - \frac{6k_B T}{[W_M + k_B T \ln(\omega\tau_0)]}, \tag{6}$$

where W_M is the maximum barrier height for hopping at infinite separation also, which is called the binding energy of the carrier in its localized sites,[27,29] k_B is the Boltzmann constant, and τ is a characteristic relaxation time which is on the order of an atom vibration period $\tau = 10^{-12}$ s. The value of W_M can be calculated according to[29]

$$s = 1 - \frac{6k_B T}{W_M}. \tag{7}$$

The value of s is in a range from 0.7 to 1.0 at room temperature, and decreases with increasing temperature according to CBH.

The hopping distance R_ω, the lower bound (cutoff) R_{min}, and the Coulombic barrier height W_m are calculated respectively from the following eauations[27,29,31–34]

$$R_\omega = \frac{e^2}{\pi\varepsilon\varepsilon_0 [W_M - k_B T \ln(1/\omega\tau_0)]}, \tag{8}$$

where e is the electronic charge and ε is the dielectric constant of material

$$R_{min} = \frac{e^2}{\pi\varepsilon\varepsilon_0 W_M}, \tag{9}$$

$$W_m = W_M - \frac{e^2}{\pi\varepsilon\varepsilon_0 R_\omega}. \tag{10}$$

According to the Austin–Mott formula based on the CBH model, $\sigma_{ac}(\omega)$ can be explained in terms of hopping of electrons between pairs of localized states at Fermi level. The $\sigma_{ac}(\omega)$ is related to the density of localized states $N(E_F)$ at Fermi level, which is given by the following equation[35]

$$\sigma_{ac}(\omega) = \frac{\pi}{3} e^2 k_B T \alpha^{-5} [N(E_F)]^2 \omega \left[\ln\left(\frac{\nu_{ph}}{\omega}\right)\right]^4, \tag{11}$$

where α is the exponential decay parameter of the localized state wave function and ν_{ph} is the frequency of the phonons. The dependence of $\sigma_{ac}(T)$ on temperature was found to obey the well-known relation[13]

$$\sigma_{ac}(T) = \sigma_0 \exp\left[\frac{-\Delta E_{ac}}{k_B T}\right], \tag{12}$$

where σ_0 is the pre-exponential constant, and ΔE_{ac} is the ac-activation energy.

Electrical transport process parameters can be analyzed by complex electric modulus formalism. This presents an alternative approach based on polarization analysis. Complex electric modulus plots give more importance to elements with the smallest capacitance occurring in the dielectric system. The real and imaginary parts of the electric moduli M' and M'' can be calculated from ε_1 and ε_2 as follows:[36–38]

$$M^* = \frac{1}{\varepsilon^*} = M' + iM'', \tag{13}$$

$$M' = \frac{\varepsilon_1}{\varepsilon_1^2 + \varepsilon_2^2}, \tag{14}$$

$$M'' = \frac{\varepsilon_2}{\varepsilon_1^2 + \varepsilon_2^2}. \tag{15}$$

The temperature dependence of the characteristic relaxation time can be calculated from the Arrhenius relation[14,39]

$$\omega_{max} = \omega_0 \exp\left[\frac{-\Delta E_\omega}{k_B T}\right], \tag{16}$$

where ω_0 is the pre-exponent factor, and ΔE_ω is the activation energy for dielectric relaxation, which is about 0.21 eV.

3. Results and discussion

3.1. AC conductivity

3.1.1. Frequency-dependent conductivity

The curves of frequency dependent AC electrical conductivity, σ_{ac}, at different temperatures are shown in Fig. 3.

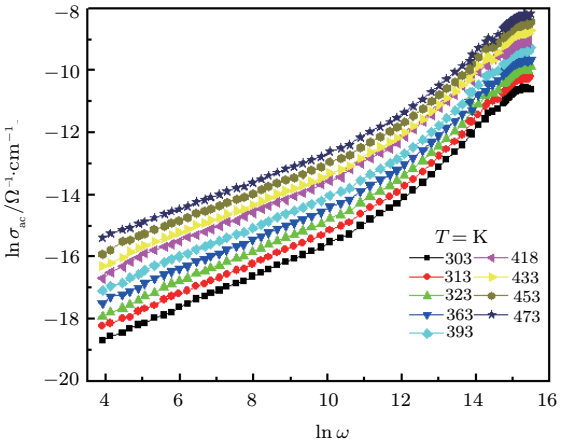


Fig. 3. (color online) The frequency dependence of σ_{ac} for PtOEPfilm as a function of temperatures.

The calculated value of s of PtOEP thin film decreases with the increase of temperature, and ranges from 0.86 to 0.97 and relates to the CBH model.[27–30]

By plotting $(1-s)$ versus T as shown in Fig. 4 and using its slope, the binding energy W_M is found to be 0.977 eV. The value of W_M is equal to the band gap E_g for the material

of conduction by bipolaron hopping. For the case of single-polaron transport, the value of W_M in the CBH mechanism is equal to one quarter of E_g.[40–43] In our case, the value of W_M is approximately a quarter of fundamental energy gap of PtOEP thin film[24] indicating that the single polaron hopping is a dominating mechanism.

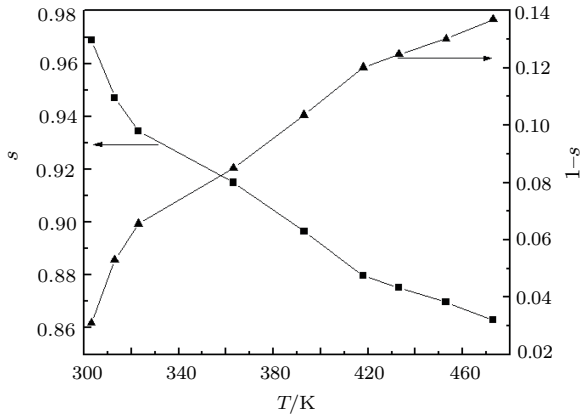


Fig. 4. The temperature dependence of s and $1-s$ for PtOEP film.

The values of R_ω, lower bound (cutoff) R_{min}, and the Coulombic barrier height W_m are given in Table 1 at various frequencies. By assuming $\nu_{ph} = 10^{12}$ Hz and $\alpha^{-1} = 10$ Å, the values of $N(E_F)$ are calculated at different frequencies (at temperature $T = 303$ K) and the results are listed in the following Table 1.

Table 1. AC conductivity parameters of PtOEP films at various frequencies ($T = 303$ K).

f/kHz	R_w/Å	R_{min}/Å	W_m/eV	$N(E_F)/10^{22}$ eV·cm^{-3}
10	3.07	1.60	4.21	1.282
1000	2.43	1.601	3.01	1.526
2000	2.39	1.602	2.82	1.645
5000	2.33	1.603	2.59	2.235

It can be observed that the values of $N(E_F)$ increase with the increase of frequency and $\sigma_{ac}(\omega)$. The increasing of the applied frequency of the electric field supports the electronic hops between localized states,[20,21,34] thus leading to the increase of the density of localized states $N(E_F)$ at Fermi level. In this case charges can hop easily at the nearest neighbor sites, so that R_ω and W_m decrease as frequency increases[38] (see Table 1).

3.1.2. Temperature-dependent conductivity

Temperature dependences of σ_{ac} of PtOEP thin films are shown in Fig. 5 at different frequencies. The activation energies of the AC conduction are calculated from the slopes of the lines. The $\ln\sigma_{ac}$ increases linearly with temperature increasing. This suggests that σ_{ac} is a thermally activated process for each of the different localized states in the gap.[44]

The frequency dependence of ΔE_{ac} is shown in Fig. 6. It is clear that the value of ΔE_{ac} decreases with the increase of applied frequency, such a behavior was observed in other organic thin films[21,45,46] and is attributed to the contribution of the frequency to the conduction mechanism, which confirms the domination of the hopping conduction mechanism.[20,21,34,45,46]

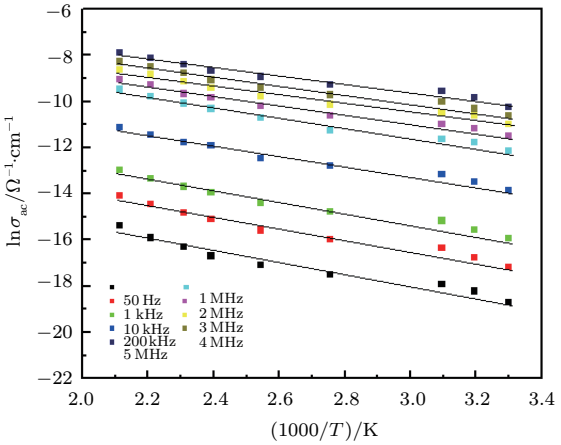


Fig. 5. (color online) The temperature dependence of $\sigma_{ac}(\omega)$ for PtOEP film as a function of frequency.

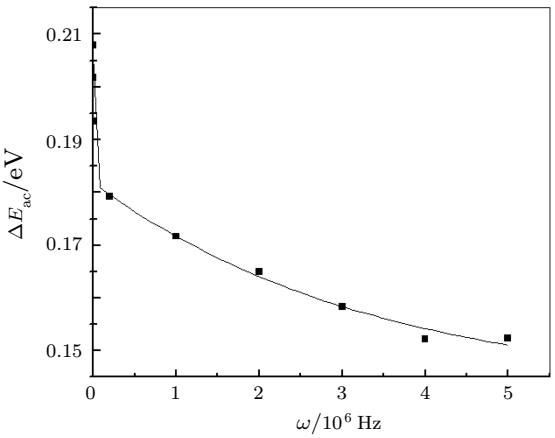


Fig. 6. The frequency dependence of $\Delta E_{ac}(\omega)$ for PtOEP film.

3.2. Dielectric properties

Dielectric studies are an essential source of valuable information about conduction processes since they can be used to recognize the origin of the dielectric losses, the electrical and dipolar relaxation time and its activation energy.[47,48] Dielectric analysis measures the electrical properties of material as a function of temperature and frequency. Two fundamental electrical characteristics of materials are defined by the dielectric analysis, i.e., (i) the capacitive insulating nature, which represents its ability to store electrical charge, and (ii) the conductive nature, which represents its ability to transfer electric charge.[49,50]

Dielectric properties of PtOEP film including dielectric constant ε_1 and dielectric loss ε_2 are studied in a frequency

range of 50 Hz–5 MHz and temperature range of 303 K–473 K. ε_1 is related to the capacitive nature of the material and is a measure of the reversible energy stored in the material by polarization, while ε_2 is a measure of the energy required for molecular motion.[51,52]

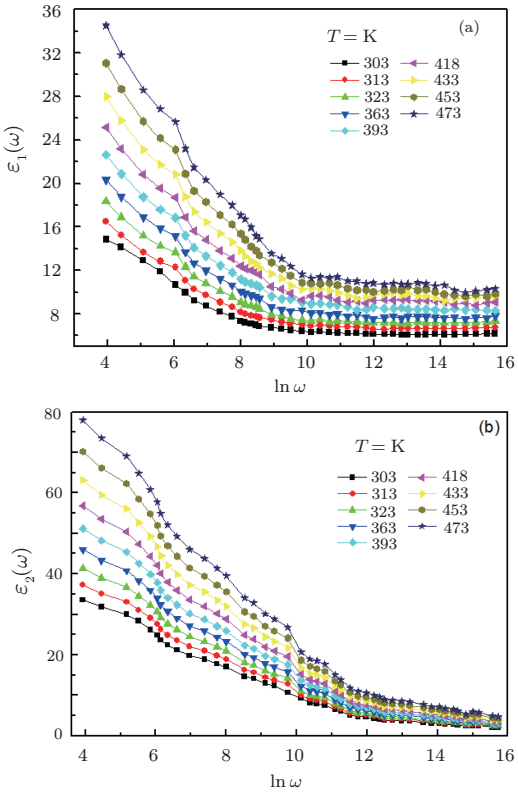


Fig. 7. (color online) The frequency dependence of ε_1 for PtOEP film as a function of temperatures.

The frequency dependences of ε_1 and ε_2 at different temperatures are illustrated in Figs. 7(a) and 7(b), respectively. Both ε_1 and ε_2 decrease with the increase of frequency. This can be explained by means of dielectric polarization.[53–59] The ε_1 and ε_2 decreasing with the increasing of frequency can be explained as follows: at low frequencies the contribution of multi-components of polarizability, deformational polarization (electronic and ionic), and relaxation polarization (orientational and interfacial) occur and this contribution leads to increases of ε_1 and ε_2 at low frequencies. Also, the dipoles align themselves along the field direction and fully contribute to the total polarization.

As the frequency increases, dipoles no longer rotate sufficiently rapidly. So, their oscillations begin to lag behind the field. As the frequency further increases, the dipole will be unable to follow the field and the orientation stops, so the contribution of the polarization becomes less. Therefore ε_1 and ε_2 decrease at a higher frequency approaching constant values due to the interfacial polarization.[58]

The temperature dependences of both ε_1 and ε_2 at different frequencies of PtOEP films are shown in Figs. 8(a) and 8(b). Both ε_1 and ε_2 increase as the temperature increases over the applied frequencies, which can be attributed to the fact that dipoles in polar materials cannot orient themselves at low temperatures while at high temperatures, the orientation polarization increases causing the dielectric constant to increase.[20,21,34,45,46]

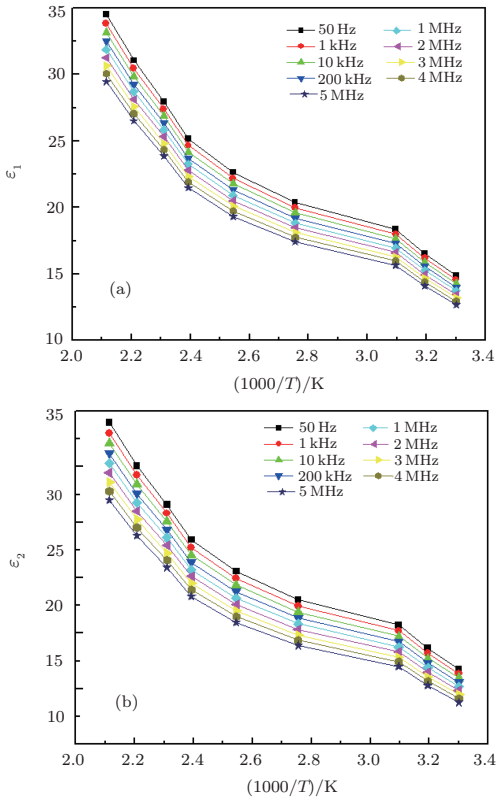


Fig. 8. (color online) The frequency dependence of ε_2 for PtOEP film as a function of temperatures.

3.3. Complex dielectric modulus

The variations of M' with frequency at different temperatures are shown in Fig. 9.

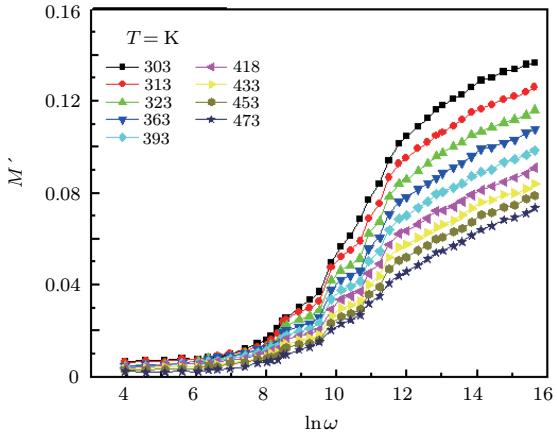


Fig. 9. (color online) The frequency dependence of M' for PtOEP film as a function of temperature.

At the low frequency region, M' values tend to zero, which confirms the negligible or absent electrode polarization

phenomenon.[38,60,61] A continuous increase of the M' dispersion with increasing frequency shows a tendency to constant values at high frequencies for all the temperatures. This behavior may be due to the short-range mobility of charge carriers.[60] M'' represents the energy loss under an electric field.[61]

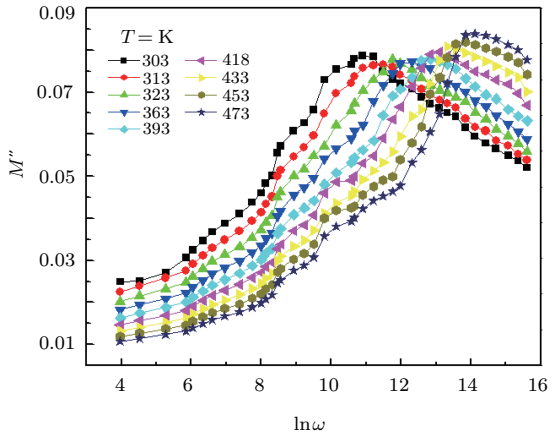


Fig. 10. (color online) The frequency dependence of M'' for PtOEP film as a function of temperature.

Figure 10 shows the plots of M'' values versus the logrithm of frequency ($\ln(\omega)$) at different temperatures. The variation of M'' with frequency shows that the relaxation peaks are moving towards higher frequencies by increasing temperature. This behavior indicates that the dielectric relaxation is thermally activated in which the hopping process of the charge carrier dominates intrinsically.[38,60–63] The asymmetric broadening of the M'' peak shows the spread of relaxation with time constant so, relaxation of our sample follows the non-Debye type.[63] The frequency region below the peak maximum is an indication of the transition from long-range to short-range mobility with the increase of frequency.[14,63]

The most suitable way to measure relaxation time is to choose the inverse of frequency of the maximum position ($\tau_{\rm m} = \omega_{\rm m}^{-1}$) as shown in Fig. 11.

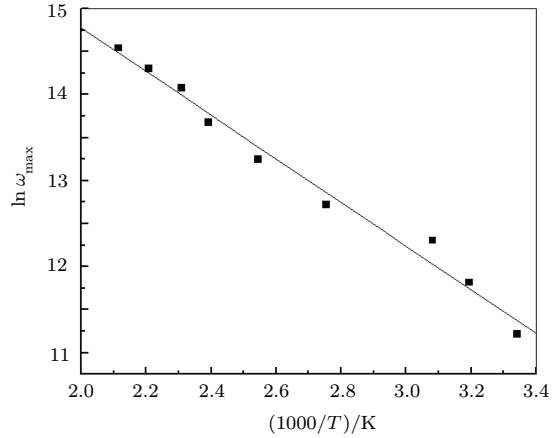


Fig. 11. The variation of $\ln \omega_{\rm max}$ versus $1000/T$ for PtOEP film.

4. Conclusions

AC conductivities and dielectric properties of nanostructured PtOEP films are studied in a temperature range of 303 K–473 K and frequency range from 50 Hz to 5 MHz. The obtained results of AC conductivity are reasonably explained in terms of the correlated barrier hopping (CBH) model. Dielectric constant ε_1 and dielectric loss ε_2 are found to decrease with frequency increasing and increase with temperature increasing in the investigated range. The real part of the modulus M' in the low frequency region tends to zero; this approves the elimination of the electrode effect in the material. The imaginary part of dielectric modulus, M'' peak shifts toward the higher frequency region with increasing temperature, specifying that the presence of dielectric relaxation is due to the thermal activiation. The dielectric relaxation time obtained from M'' shows an Arrhenius behavior with $\Delta E_\omega = 0.21$ eV.

References

[1] Trogler W C and Choy H C 2013 *Organic Solar Cells Materials and Device Physics* p. 250
[2] Dongol M, El-Denglawey A, Elhady A F and Abuelwafa A A 2015 *Appl. Phys. A* **118** 345
[3] Schon J H, Kloc C and Batlogg B 2001 *Phys. Rev. Lett.* **86** 3843
[4] Perepichka D F, BryceM R, Batsanov A S, McInnes E J L, Zhao J P and Farley R D 2002 *Chem. Eur. J.* **8** 4656
[5] Brütting W 2005 *Physics of Organic Semiconductors* (WILEY-VCH: Verlag GmbH & Co. KGaA)
[6] Toal S J and Trogler W C 2006 *J. Mater. Chem.* **16** 2871
[7] Dongol M, El-Nahass M M, El-Denglawey A, Elhady A F and Abuelwafa A A 2012 *Curr. Appl. Phys.* **12** 1178
[8] Dongol M, El-Denglawey A, Elhady A F and Abuelwafa A A 2012 *Curr. Appl. Phys.* **12** 1334
[9] Li X, Zhang C, Wu Y, Zhang H, Wang W, Yuan L, Yang H, Liu Z and Chen H 2015 *Int. J. Mol. Sci.* **16** 27707
[10] Lee C, Hwang I, Byeon C C, Kim B H and Greenham N C 2010 *Adv. Funct. Mater.* **20** 2945
[11] Tsuboi T, Wasai Y and Gabain N 2006 *Thin Solid Films* **496** 674
[12] Xiong K, Hou L, Wang P, Xia Y, Chen D and Xiao B 2014 *J. Lumin.* **151** 193
[13] Eldenglawey A 2013 *Structural, optical and electrical properties of As-Se-Tl films: Physical properties of As-Se-Tl films* (LAP LAMBERT Academic Publishing) p. 85
[14] Darwish A A A, El-Nahass M M and Bekheet A E 2014 *J. Alloys Compd.* **586** 142
[15] Mohamed R I 2000 *J. Phys. Chem. Solids* **61** 1357
[16] El-Nahass M M, Atta A A, Kamel M A and Huthaily S Y 2013 *Vacuum* **91** 14
[17] Elliott S R 1979 *Phil. Mag. B* **40** 507
[18] Zeyada H M, El-Nahass M M and Makhlouf M M 2011 *Curr. Appl. Phys.* **11** 1326
[19] El-Nahass M M, Metwally H S, El-Sayed H E A and Hassanien A M 2012 *Mater. Chem. Phys.* **133** 649
[20] El-Nahass M M, Farag A A M, Abu-Samaha F S H and Elesh E 2014 *Vacuum* **99** 153
[21] El-Nahass M M, Atta A A, El-Zaidia E F M, Farag A A M and Ammar A H 2014 *Mater. Chem. Phys.* **143** 490
[22] Nawar A M, Abd El-Khalek H M and El-Nahass M M 2015 *Org. Opto-Elect.* **1** 25
[23] Abuelwafaa A A, El-Denglawey A, Dongol M, El-Nahass M M and Soga T 2016 *J. Alloys Compd.* **655** 415
[24] Abuelwafaa A A, El-Denglawey A, Dongol M, El-Nahass M M and Soga T 2015 *Opt. Mater.* **49** 271
[25] Tolansky T 1948 *Multiple-Beam Interferometry of Surface and Films* (London: Oxford University Press) p. 125
[26] Jonscher A K 1977 *Nature* **267** 673

[27] Elliott S R 1987 *Adv. Phys.* **36** 135
[28] Long A R 1982 *Adv. Phys.* **31** 553
[29] Elliott S R 1977 *Philos. Mag. B* **36** 1291
[30] Elliott S R 1978 *Philos. Mag. B* **37** 135
[31] Shimakawa K and Kondo A 1983 *Phys. Rev. B* **72** 1136
[32] Pike G E 1972 *Phys. Rev. B* **6** 1572
[33] Atyia H E 2014 *Acta Phys. Pol. A* **125** 98
[34] Kahouli A, Sylvestre A, Jomni F, Yangui B and Legrand J 2012 *J. Phys. Chem. A* **116** 1051
[35] Austin I G and Mott N F 1969 *Adv. Phys.* **18** 41
[36] Macedo P B, Moynihan C T and Laberge N L 1973 *Phys. Chem. Glasses* **14** 122
[37] Macedo P B, Moynihan C T and Bose R 1972 *Phys. Chem. Glasses* **13** 171
[38] Wonga Y J, Hassan J and Hashim M 2013 *J. Alloys Compd.* **571** 138
[39] El-Nahass M M and Ali H A M 2012 *Solid State Commun.* **152** 1084
[40] Dakhel A A 2006 *Thin Solid Films* **496** 353
[41] Chen R H, Chang R Y and Shern S C 2002 *J. Phys. Chem. Solids* **63** 2069
[42] Chen R H, Shern S C and Fukami T 2002 *J. Phys. Chem. Solids* **63** 203
[43] Farag A A M, Mansour A M, Ammar A H, Abdel Rafea M and Farid A M 2012 *J. Alloys Compd.* **513** 404
[44] Yakuphanoglu F, Aydogdu Y, Schatzschneider U and Rentschler E 2003 *Solid State Commun.* **128** 63
[45] El-Menyawy E M, Zeyada H M and El-Nahass M M 2010 *Solid State Sci.* **12** 2182
[46] El-Nahass M M, Kamal H, Elshorbagy M H and Abdel-Hady K 2013 *Org. Electron.* **14** 2847
[47] Ayouchi R, Leien D, Martin F, Gabas M, Dalchiele E and Barrodo J R 2003 *Thin Solid Films* **68** 426
[48] Rhouma F H I, Dhahri A, Dhahri J and Valente M A 2012 *Appl. Phys. A* **108** 593
[49] Hegab N A and El-Mallah H M 2009 *Acta Phys. Pol. A* **116** 1048
[50] Atyia H E Hegab N A, Affi M A and Ismail M A 2013 *J. Alloys Compd.* **574** 345
[51] Atyia H E 2014 *J. Nonlinear Cryst. Solids* **391** 83
[52] Atyia H E, Farid A M and Hegab N A 2008 *Physica B* **403** 3980
[53] Yahia I S, Hegab N A, Shakra A M and AL-Ribaty A M 2012 *Physica B* **407** 2476
[54] Stevels J M 1975 *Handbuch der Physik. In: Flugge* (Berlin: Springer) p. 108
[55] El-Nahass M M, Ali H A M, Saadeldin M and Zaghllol M 2012 *Physica B* **407** 4453
[56] Smyth P 1965 *Dielectric Behavior and Structure* (New York: McGraw-Hill)
[57] Barsoum M 1997 *Fundamental of Ceramics* (London: McGraw Hill) p. 215
[58] Tareev B 1975 *Physics of Dielectric Materials* (Moscow: Mir Publishers) p. 187
[59] Sharma A and Mehtaa N 2012 *Eur. Phys. J. Appl. Phys.* **59** 10101
[60] Tabib A, Sdiri N, Elhouichet H and Fe'rid M 2015 *J. Alloys Compd.* **622** 138
[61] Dult M, Kundu R S, Hooda J, Murugavel S, Punia R and Kishore N 2015 *J. Non-Cryst. Solids* **423–424** 1
[62] Atif M and Nadeem M 2015 *J. Alloys Compd.* **623** 447
[63] El-Menyawy E M, Zedan I T, Mansour A M and Nawar H H 2014 *J. Alloys Compd.* **611** 50